R-4629

UCRL-53098

MASTER

# National Seismic Stations Transducers and Filters

P. W. Rodgers
M. Hummell

January 13, 1981

Lawrence Livermore National Laboratory

Test Ban Treaty Verification Program

DISTRIBUTION OF THIS DOCUMENT IS UNLIMITED

UCRL-53098
Distribution Category UC-11

# National Seismic Stations Transducers and Filters

P. W. Rodgers
M. Hummell

Manuscript date: January 13, 1981

DISCLAIMER

LAWRENCE LIVERMORE LABORATORY
University of California • Livermore, California • 94550

Available from: National Technical Information Service • U.S. Department of Commerce
5285 Port Royal Road • Springfield, VA 22161 • $6.00 per copy • (Microfiche $3.50)

# CONTENTS

# National Seismic Stations Transducers and Filters


## ABSTRACT

The National Seismic Stations (NSS) instruments are being developed for seismic monitoring of regional and teleseismic events. They consist of two 3-component, broadband, borehole seismometers: the KS-36000 and the S-700, which is the backup for the KS-36000. Output is divided into frequency bands to reduce data loss due to saturation.

Complete block diagrams of the KS-36000 and S-700 NSS seismometers and filters are presented. Both open-loop and closed-loop steady-state amplitude and phase curves are given. Without band-pass filters (but with shaping filters) the KS-36000 has a flat (i.e., between the -3dB points) velocity sensitivity from 0.03 to 23 Hz. With its shaping filters, the S-700 is flat from 0.2 to 40 Hz. The structure of the three band-pass filters (LP, MP, and SP) is superimposed on these velocity sensitivities. Passbands of the resulting overall velocity sensitivity for the KS-36000 are as follows: LP band = 0.01-0.05 Hz, MP band = 0.02-1.3 Hz, and SP band = 1-10 Hz. Step-function responses and phase and group delays are given for each of the bands. The MP-band step response is oscillatory due to its sharp, high-frequency cutoff, but an MP-band filter with a less abrupt cutoff eliminates the oscillation.

To generate typical NSS output seismograms, velocity inputs from [illegible] representative seismic events were used: an underground nuclear test (Δ ≈ 3.6 [illegible]), a regional earthquake (Δ ≈ 20 [illegible]), a local earthquake (Δ ≈ 1.5 [illegible]), and a teleseismic earthquake (Δ ≈ [illegible] 23 [illegible]). The velocity inputs for these events were obtained from the LLNL digital seismic network (DSS) around the Nevada Test Site (NTS). The seismograms resulting [illegible] of the bands were satisfactory, although the low-frequency [illegible] of the MP [illegible] creased in frequency to 0.08 Hz.

The S-700 with an open-loop resonant frequency of [illegible] Hz [illegible] specification at 1 Hz. We therefore recommend that the S-700 [illegible] conventional short-period seismometer such as the Mark Products L-4.


## CHAPTER 1: INTRODUCTION

N[illegible] S[illegible] S[illegible] (NSS) [illegible] are being developed [illegible] ing of regional [illegible] teleseismic events. [illegible] sited in boreholes [illegible] tances from [illegible] under [illegible]

NSS [illegible] NSS [illegible] scale [illegible] seismic events [illegible] local events [illegible] frequency teleseismic events. The broadband [illegible] puts of NSS seismometers [illegible] separ[illegible] in boreholes to reduce seismic noise. Three components are used because they greatly increase the ability to identify particular wave types.

This report presents the steady-state sinusoidal and dynamic responses of both NSS seismometers. The block diagram of each instrument and filter is given, and corresponding analytic transfer functions are contained in the Appendices.

Both open- and closed-loop frequency responses are plotted for the two transducers. Overall (including filters) velocity sensitivity* (VS) curves together with phase and group delays are also presented.

The dynamic response of each seismometer and filter combination is shown both by its response to a step function in velocity and its response to seismic inputs. Representative seismic inputs are velocitygrams of local, regional, and teleseismic events as recorded by the LLNL digital seismic network.

Data for these computations were taken from the August 11, 1979 and February 27, 1980 informal reports of H. B. Durham (Sandia): "NSS-Model II, Seismic Data System Response Functions." Transfer functions for the S-700 were taken from the latter report and those for the KS-36000 from the former; therefore the responses for the KS-36000 are slightly, but not significantly, different from the current version.

# CHAPTER 2: THE KS-36000

## OVERALL BLOCK DIAGRAM

The overall block diagram for the KS-36000 is shown in Fig. 1. The transducer itself is block $H_T$, which is further broken down into its internal feedback loop. Transfer functions for $H_T$, $H_A$, $H_B$, and $K_T$ are given in Appendix A. $H_T$ is followed by the Long Period Mid Period (LP MP) shaping filter, $H_{S1}$, and the Short Period (SP) shaping filter $H_{S2}$. Transfer functions for $H_{S1}$ and $H_{S2}$ are also given in Appendix A. The two shaping filters feed into the

* [illegible]

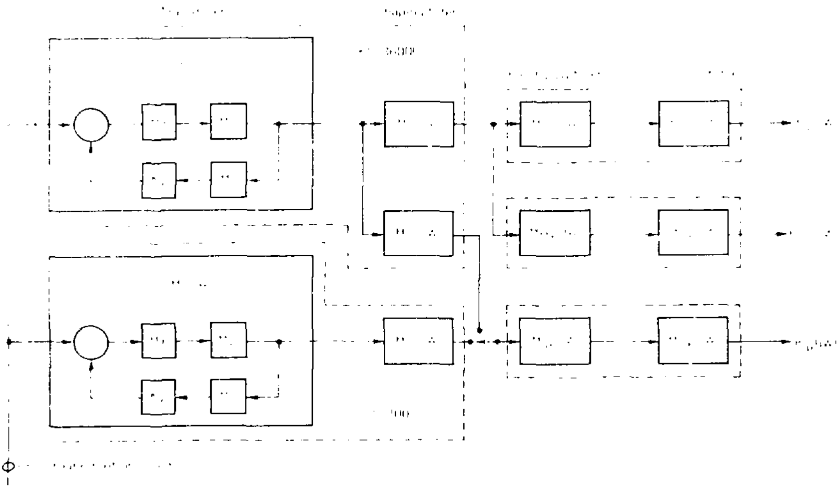

FIG. 1. Overall block diagram for NSS seismographs showing feedback loops for the transducers, shaping filters, band-pass filters, and common filters.

three major band-pass filters $H_{LP}$, $H_{MP}$, and $H_{SP}$ which, in turn, are followed by the three common filters, $H_{CF}$. Transfer functions for the band-pass and common filters are listed in Appendix B.

## TRANSDUCER CHARACTERISTICS

The open-loop frequency-response curve, $H_T H_A H_V K_F$ is given in Fig. 2. The peak at approximately 0.2 Hz is due to the resonance of the lightly damped ($\xi$ = 0.01417) spring-mass system of the seismometer itself. The closed-loop acceleration response which is flat out to 23 Hz (–3dB) with a corner frequency at approximately 30 Hz is shown in Fig. 3.

## SHAPING FILTERS

Figures 4 and 5 show the frequency response of the two shaping filters, $H_{S1}$ and $H_{S2}$. The purpose of $H_{S1}$ is to cause the VS curve of $H_1$ to fall off as $\sim f^3$ at frequencies below 0.01 Hz. (Without $H_{S1}$, it would fall off as f.) The resulting overall VS curve for the transducer ($sH_1$ $H_{S1}$) is shown in Fig. 6. It rises with a +3 slope (corresponding to $f^3$) below its low-frequency corner at 0.0105 Hz (= 1/95 sec). It is then flat out to approximately 20 Hz where it falls off with a –4 slope. The frequency response of LP and MP bands will be superimposed on this curve to obtain the overall VS curves for the KS-36000.

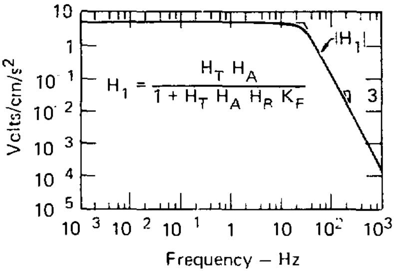


**FIG. 3. KS-36000 closed loop acceleration response is flat to 23 Hz.**

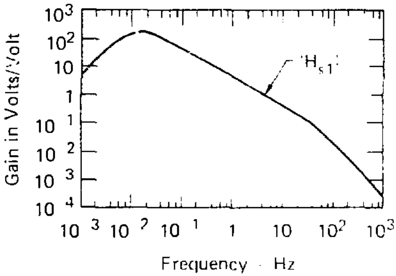


**FIG. 4. Shaping filter, $H_{S1}$, frequency response.**

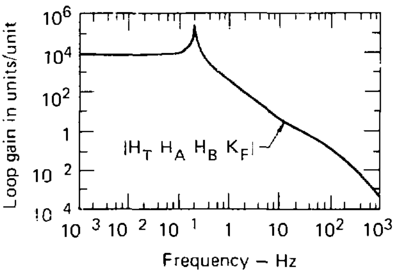


**FIG. 2. KS-36000 open-loop frequency-response curve peaks at approximately 0.2 Hz due to mechanical resonance of the pendulum.**

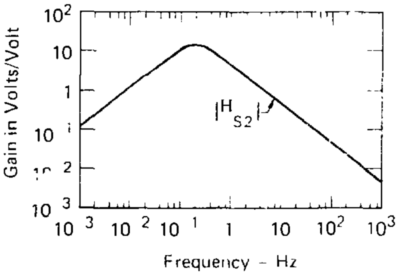


**FIG. 5. Shaping filter, $H_{S2}$, frequency response.**

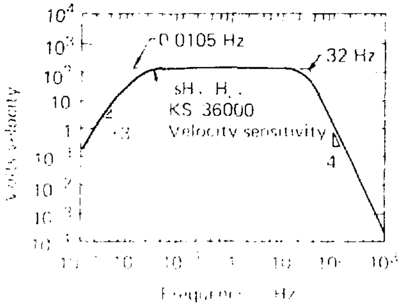


FIG. 6. KS-36000 velocity sensitivity without band filters for LP and MP bands.

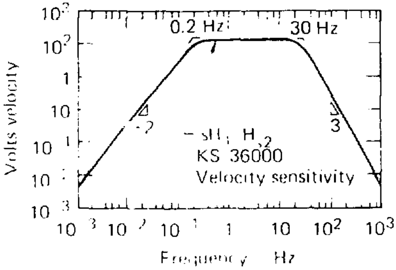


FIG. 7. KS-36000 velocity sensitivity without band filters for SP band.

[illegible] KS-36000 [illegible] SP [illegible] 30 Hz SP pass[illegible] will be imposed on this response to obtain the overall SP VS.

To summarize, the two important curves are those of Figs. 6 and 7 which characterize the VS of the KS-36000.

# CHAPTER 3: THE S-700

[illegible] response of the S-700 seismometer [illegible] KS-36000 [illegible] Appendix A [illegible] KS-36000 [illegible]

30 Hz. The peaked shape [illegible] response of [illegible] the shaping filter [illegible] The resulting overall VS for the S-700 [illegible] approximately 0.2 to 30 Hz. Whether [illegible] S-700 response will [illegible] 0.2 Hz [illegible] very much depend [illegible] noise in that region. The characteristics of the SP filter will be combined with this response to develop the overall VS for the S-700 [illegible] through the SP filter [illegible] LP or MP [illegible] the S-700.

# CHAPTER 4: BAND-PASS FILTER CHARACTERISTICS

As was shown in the NSS block diagram, outputs of the KS-36000 and the S-700 are shaped by passing them through the three band-pass filters LP, MP and SP. Before describing these filters in detail it is worthwhile to review some general characteristics of filter types used in the NSS.

## PROPERTIES OF BAND-PASS FILTERS

Filters discussed in this section are all of the band-pass type. They are described in terms of some

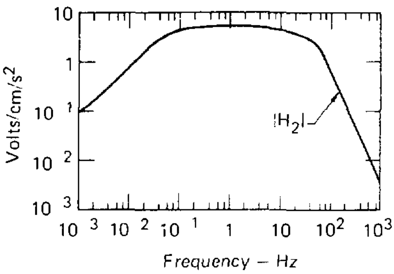


FIG. 8. S-700 closed-loop acceleration response.

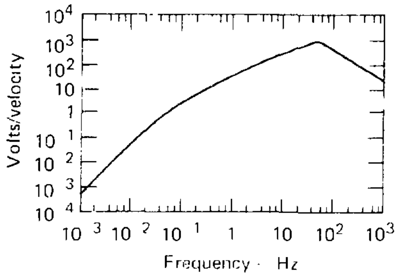


FIG. 9. S-700 closed-loop velocity response.

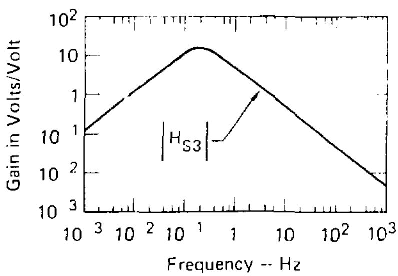


FIG. 10. Shaping filter, $H_{S3}$ for S-700.

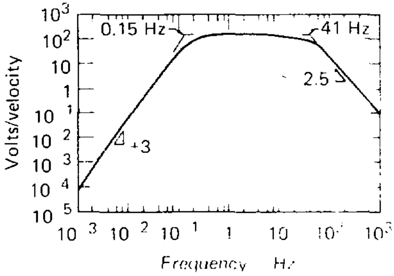


FIG. 11. Overall velocity sensitivity for S-700.

combination of their transfer function, frequency and phase response, and step-function response.

Some general properties of [illegible] filters are as follows:

1. The sharper the filter corner, the greater the tendency for ringing in its step-function response.

2. *In general, for broad band-pass filters* the rise time of the step-function response is determined by the high-frequency corner and [illegible] the low-frequency corner.

3. The more the phase response [illegible] frequency departs from a linear [illegible] phase distortion or dispersion results.

4. In general, [illegible] the higher the Q, the greater [illegible] filter to ring.

## TYPES OF CLASSICAL ANALOG FILTERS

Three types of analog filters [illegible] seismic filters are as follows:

1. Simple filters. All poles [illegible] negative real axis of the s plane [illegible] critically damped or overdamped [illegible] could be considered to be a second-order* [illegible] filter.

2. Butterworth filters. All poles [illegible] semicircle in the left half of the s-plane. The amplitude spectrum is very flat and has a relatively sharp corner.

*The order [illegible] describing [illegible]

**TABLE 1. Summary of simple, Butterworth, and Bessel filter characteristics.**

| | Simple filter | Butterworth filter | Bessel filter |
|---|---|---|---|
| Shape of spectral amplitude response | Moderately flat, moderately rounded corner | Very flat, sharp corner | Very sloping, very rounded corner |
| Overshoot in step response | None | Moderate | Very little |
| Phase distortion | Moderate | Quite a bit | Least |

3. Bessel filters. These filters tend to approximate a linear phase response and thus exhibit minimum phase distortion or dispersion. The amplitude spectrum is quite sloped with a very rounded corner.

Based on the above descriptions, the simple filter can be regarded as midway between the Butterworth and the Bessel filter.

A fourth type of filter, the Chebyshev, is not used in frequently in seismic instruments because its amplitude spectrum is not smooth and its step response has a large overshoot.

Table 1 shows that none of the filters exhibits all three desirable qualities of near rectangular passband, no overshoot in step response, and linear phase. From the viewpoint of selectively rejecting noise in a stop band[3] and passing signal in another (a near-rectangular passband), the Butterworth filter is desirable. But with regard to deconvolving seismic data, freedom from overshoot and dispersion is important. It is also desirable to minimize the number of poles to reduce the phase distortion. These tradeoffs will be referred to again when discussing the details of the NSS passbands.

# CHAPTER 5: NSS BAND-PASS FILTERS

## BAND FILTERS

To lessen the chances of saturation of the electronics during large seismic events, it is desirable to split up the KS-36000 and S-700 output into bands. For example, if there were only one band (a so-called broadband system), the large amplitude surface waves generated by a major, remote earthquake could cause saturation of the electronics and loss of all signals during the period of the saturation. By breaking the output into bands, presumably only the LP band would experience electronic saturation, although mechanical or electrical saturation of the transducer would spoil the data in all three bands.

## SANDIA FILTERS

Amplitude spectra of LP, MP, and SP filters proposed by Durham of Sandia (op. cit.) are shown in Fig. 12 and their transfer functions are given in Appendix B.

The LP band of the SLP is essentially the same as that of the SRO. It consists of a 2nd-order,

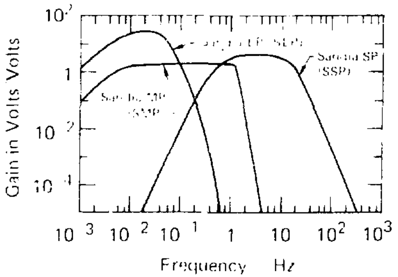


**FIG. 12. Sandia LP, MP, and SP band filter amplitude spectra.**

simple high-pass section at 0.005 Hz followed by a series of low-pass sections which result in a 12th-order rolloff (slope of -12). The result is the narrow LP band shown in Fig. 12, which is centered on 0.02 Hz (= 1/50 sec).

The MP band is a broad, flat band running from approximately 0.02 to 1.3 Hz bracketing the microseism band. It begins at low frequencies with the same 2nd-order simple high-pass section at 0.005 Hz as the LP filter. This is followed by a sharply breaking 10th-order Butterworth low-pass filter at 1.3 Hz. These in turn are followed by simple low-pass sections at 30 and 100 Hz. Since the high-pass section is 2nd order and the low-pass section 10th order (below 30 Hz), the result is the broad, asymmetric curve labeled SMP in Fig. 12.

The SP band [illegible] approximately 1 to 10 Hz. [illegible] 2nd-order simple high-pass section [illegible] 4th-order Butterworth [illegible] high-frequency [illegible] symmetrical SP [illegible] SSP [illegible] Fig. 12.

[illegible] NSS [illegible] LP, MP, and SP [illegible] filter. The [illegible] Fig. 12 are made the [illegible] high-frequency [illegible] 200 Hz [illegible] frequencies [illegible]

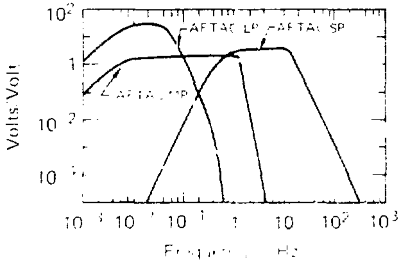


**FIG. 13 AFTAC LP, MP, and SP band filter amplitude spectra.**

dropping [illegible] SP [illegible] of the system.

## AFTAC FILTERS

AFTAC [illegible] Fig. 13 [illegible] AFTAC [illegible] Sandia [illegible] SP [illegible]

# CHAPTER 6: NSS OVERALL RESPONSES INCLUDING TRANSDUCERS AND BAND-PASS FILTERS

[illegible] example, the KS-36000 VS for the LP and MP bands [illegible] the LP and MP band transfer functions shown in Fig. 12 [illegible] SP VS [illegible] Fig. 7 is multiplied by the SP transfer function also shown in Fig. 12. The overall VS relates [illegible] the transducer to volts out of the common filter, [illegible] which is the last filter in each of the band-pass filters.

Although each of the band filters has an absolute gain associated with it, this discussion is [illegible]

[illegible]

## PROPERTIES OF THE KS-36000 WITH SANDIA FILTERS

### Velocity Sensitivity

The [illegible] KS-36000 and [illegible] VS is shown in Fig. 14 [illegible] proposed Sandia filters. The resulting curves are similar to those of

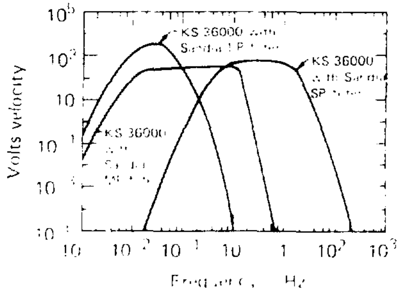


**FIG. 14 Velocity sensitivity with filters: Sandia LP, Sandia MP, and Sandia SP.**

F[illegible] filters [illegible] except for the regions of [illegible] where the KS-36000 VS [illegible]. In those regions the [illegible] shape [illegible] the KS-36000 response [illegible].

[illegible] 3dB points for this [illegible] are:

- LP Band 0.0060-0.08 Hz
- MP Band 0.02 – 3 Hz
- SP Band 1-10 Hz

## Phase Response φ(f)

The phase response accompanying the VS [illegible] in Fig. 15 for the three Sandia filters. The phase response of the SSP was begun arbitrarily at [illegible] degrees for low frequencies, and the other two phase responses were plotted accordingly. It should be noted that there is a hump at the MP curve near 1 Hz. This is due to the sharp, high-frequency corner of the MP filter. Although it is difficult to envision from semilog plots, the closer the phase response [illegible] near [illegible] frequency, the less distortion of signals passed.

## Group Delays

Group delay $\tau_{gr}$ is the delay which would be experienced by a wave packet. It is calculated from the phase delay, φ(f), by the relation

$$\tau_{gr} = \frac{d\phi(f)}{d\omega} = \frac{1}{2\pi}\frac{d\phi(f)}{df} \qquad (1)$$

It is useful to examine group delay since minima would result in large amplitude waves known as Airy phases, which distort the seismogram. Of course, onset times are also retarded by the group delay associated with the particular period of arrival.

Group delays of the KS-36000 with Sandia filters are shown in Fig. 16. The delays are large at low frequencies and approach zero at very high frequencies. Since the slopes of phase delay curves decrease in proceeding through the SP, MP, and LP bands, group delays proceed in the same order, with the largest delays associated with the LP [illegible]. Since [illegible] relatively clear [illegible] of the [illegible] slope of the phase-delay curve occurs near the corner frequency of a filter, minima seen in Fig. 16 can be associated with a particular corner frequency, and the size of the group delays is [illegible] to the [illegible] poles.

## Step Responses

St[illegible] responses [illegible] KS-36000 [illegible] LP, MP, [illegible] SP filters [illegible] Hz [illegible] Fig. 17. The [illegible] SP [illegible] LP [illegible] MP response. [illegible] MP [illegible] response [illegible].

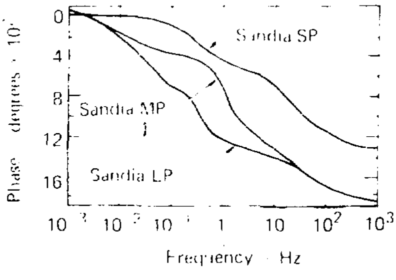


**FIG. 15. Phase response of KS-36000 with Sandia filters.**

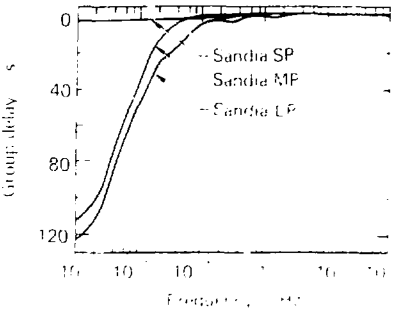


FIG. 16. Group delay of KS-36000 with Sandia filters.

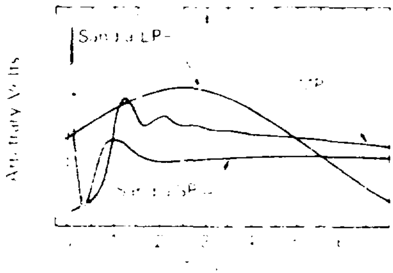


FIG. 17. Step responses of KS-36000 with Sandia filters.

[illegible]

## PROPERTIES OF THE KS-36000 WITH AELAC FILTERS

### Velocity Sensitivity Curves

[illegible]

### Step-Function Response

[illegible]

### Phase and Group Delay

The resulting SP [illegible] than with the Sandia filter [illegible] Butterworth corner. The phase [illegible] for the KS-36000 with AELAC filters [illegible] Appendix C, Figs. C1 and C2.

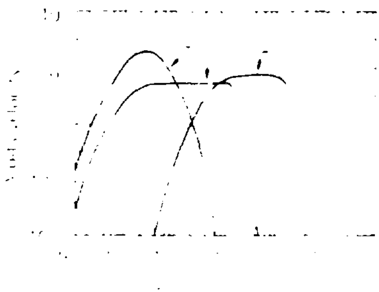

FIG. 18. Velocity sensitivity with filters AELAC LP, AELAC MP and AELAC SP.

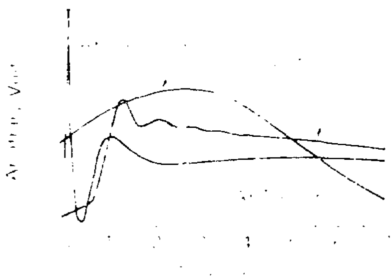

FIG. 19. Step responses of KS-36000 with AELAC filters.

# CHAPTER 7: THE MP-BAND FILTER

As was stated previously, the upper corner of the Sandia MP-band filter is abrupt. It consists of a 10th-order Butterworth filter at 1.3 Hz. This results in the oscillatory step response for the MP band shown in Figs. 17 and 18. Because this is undesirable, it is worthwhile considering two other low-pass filters for the high frequency corner of the MP band. One is a 4th-order Butterworth also cornered at 1.3 Hz. The other is a 4th-order Bessel with the same corner frequency. The corresponding VS curves for the three filters are shown in Fig. 20. Note that the Bessel is the more rounded curve. Corresponding phase and group delays appear in Figs. 21 and 22. Here group delays are shown with an expanded scale. The minima in group delay for the 10th-order Butterworth is considerably greater than that for the 4th-order Butterworth. There is almost no minimum associated with the Bessel filter because of its nearly linear phase response (which is difficult to see in Fig. 21 because the horizontal axis is logarithmic).

Figure 23 compares the step-function responses of the three filters. The three different degrees of oscillation are in the order expected for each of the filter types. From this figure it is clear that the Bessel filter outperforms the Butterworth because of its improved transient behavior.

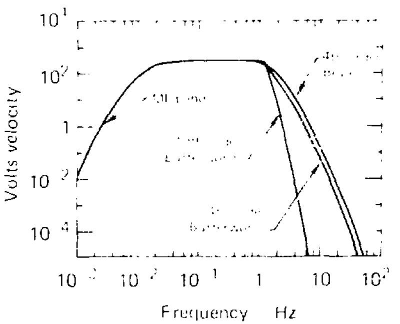


**FIG. 20. Frequency response comparison of three MP band low pass filters.**

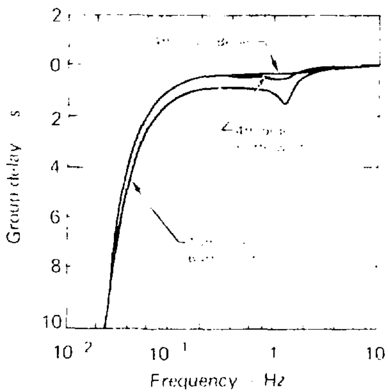


**FIG. 22. Group delay comparison of three MP band low pass filters.**

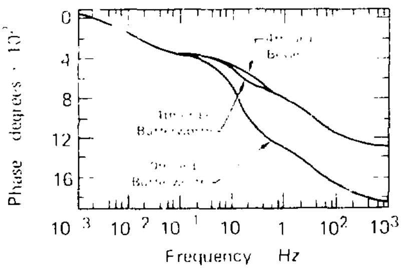


**FIG. 21. Phase delay comparison of three MP band low pass filters.**

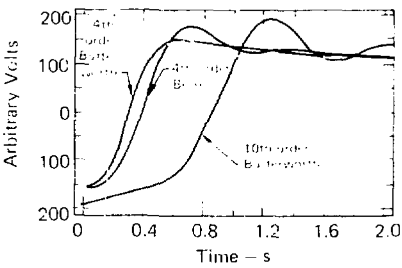


**FIG. 23. Step response comparison of three MP band low pass filters.**

# CHAPTER 8: THE KS-36000 RESPONSE TO VARIOUS REAL SEISMIC SOURCES

To develop an understanding of the significant differences in passbands, four actual seismic inputs are used as a data base to calculate outputs of the three NSS passbands. The four inputs are all vertical ground velocity [illegible] from two of the four DSS [illegible] NTS. These events [illegible] NS response [illegible] system [illegible] 24. [illegible]

[illegible]

## EVENT (i): UNDERGROUND NUCLEAR SHOT (Δ ≈ 3.6°)

[illegible] SP, MP [illegible] LP [illegible] SP, MP, and LP [illegible] spectra [illegible] LP [illegible] expected [illegible] several seconds [illegible] MP [illegible] broadband [illegible] H.

## EVENT (ii): REGIONAL EARTHQUAKE (Δ ≈ 20°)

The [illegible] 26 [illegible] range of regional distances, its distinct phases, and

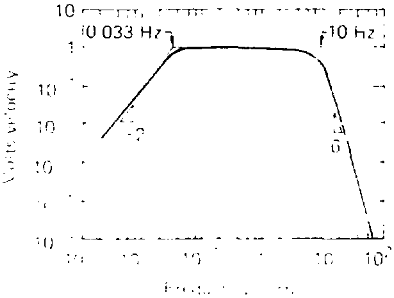


FIG. 24. DSS normalized velocity sensitivity.

[illegible] NSS [illegible] MP [illegible]

## EVENT (iii): LOCAL EARTHQUAKE (Δ ≈ 1.5°)

[illegible] MP [illegible]

## EVENT (iv): LARGE TELESEISM (Δ ≈ 123°)

[illegible] The [illegible] expected [illegible] broadband trace [illegible] D4

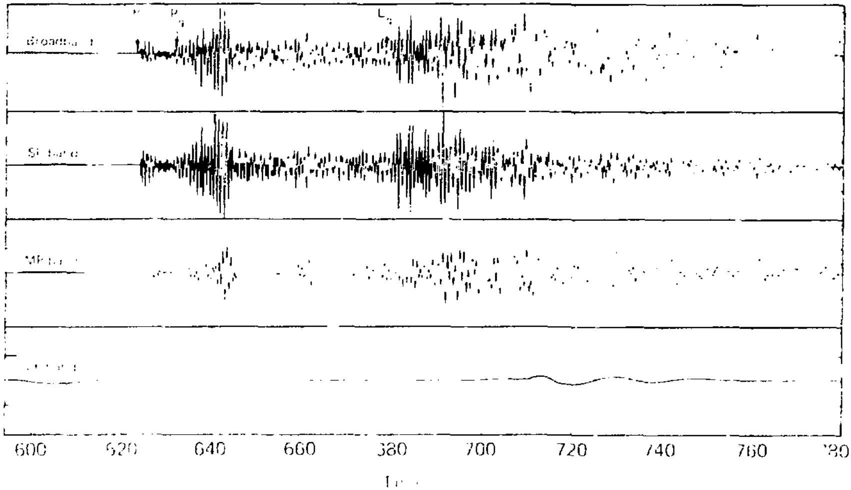


FIG. 25. Event (i): underground nuclear shot (Δ ≈ 6°).

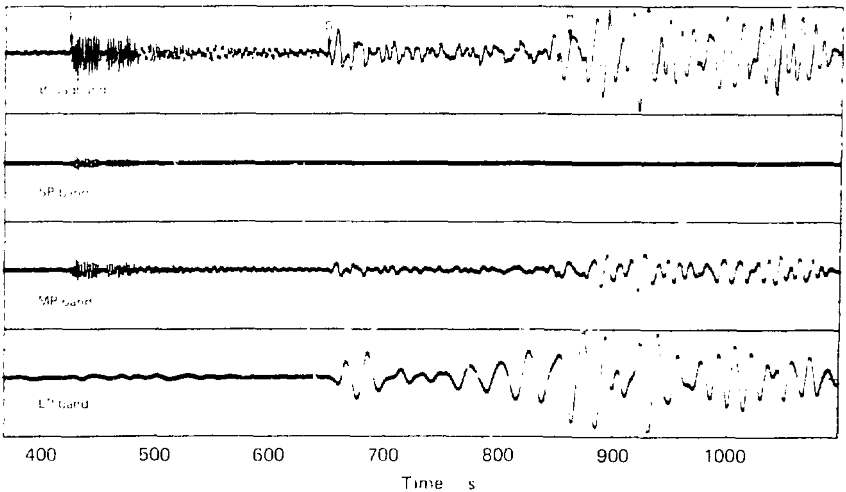


FIG. 26. Event (ii): regional earthquake (Δ ≈ 20°).

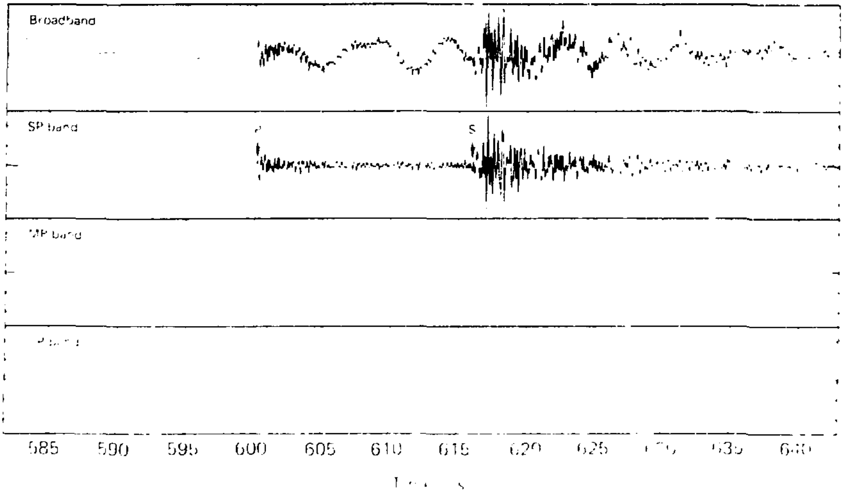


FIG. 27. Event ... local earthquake ... 1.5

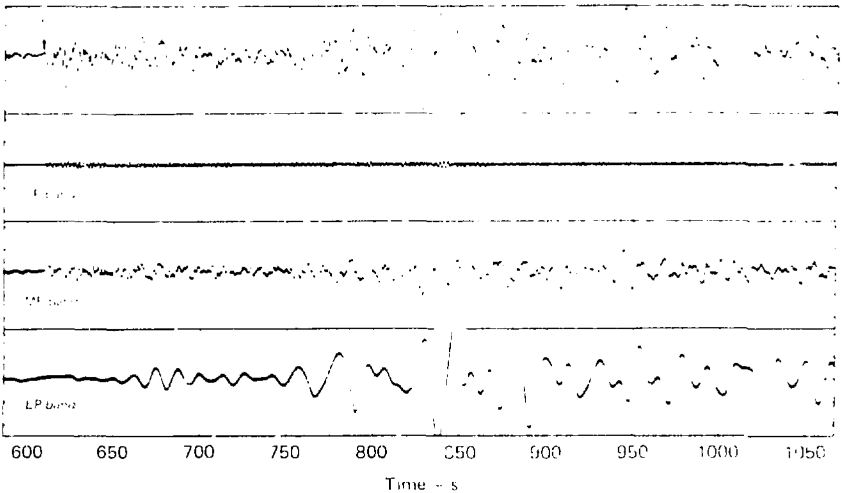


FIG. 28. Event (iv): large teleseism (Δ ≈ 123°).

## TWO MP FILTERS

## CONCLUSIONS REGARDING NSS BAND STRUCTURE

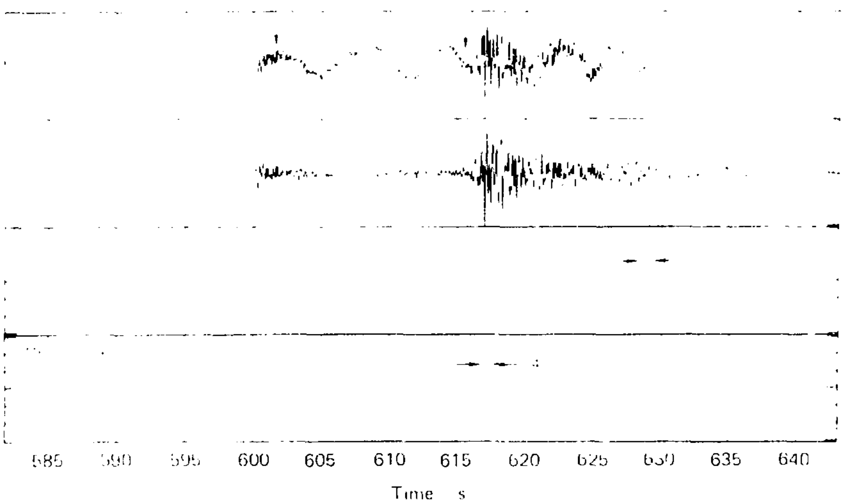


FIG. 29. Effect of two MP filters on a local earthquake.

# CHAPTER 9: THE S-700 SYSTEM

## S-700 RESPONSE TO REAL INPUTS

## S-700 RESOLUTION AND NOISE

# CHAPTER 10: GENERAL COMMENTS

## GENERAL CONFIGURATION OF THE KS-36000

## BAND STRUCTURE

## THE S-700

# ACKNOWLEDGMENT

The authors wish to acknowledge the many helpful discussions and criticisms by F. Followill, W. J. Hannon, M. Denny, and P. Moulthrop.

# APPENDIX A: SEISMOMETER TRANSFER FUNCTIONS

## TRANSFER FUNCTIONS FOR THE KS-36000 SEISMOMETER

[illegible]

## TRANSFER FUNCTIONS FOR THE KS-36000 LP AND MP SHAPING FILTERS

[illegible]

## TRANSFER FUNCTIONS FOR THE KS-36000 AND S-700 SP SHAPING FILTERS

[illegible]

[illegible]

## TRANSFER FUNCTIONS FOR THE S-700 SEISMOMETER

[illegible]

[illegible]

[illegible]

[illegible]

[illegible]

[illegible]

[illegible]

[illegible]

# APPENDIX B: FILTER TRANSFER FUNCTIONS

## SHORT PERIOD FILTER TRANSFER FUNCTIONS

[illegible]

a) [illegible]

b) [illegible]

c) [illegible]

d) [illegible]

## COMMON FILTER TRANSFER FUNCTION

[illegible]

## MID PERIOD FILTER TRANSFER FUNCTIONS

[illegible]

a) [illegible]

b) [illegible]

c) $H_C(s) = \dfrac{1.0}{1.0 + 0.0773\,s + 0.01499\,s^2}$

d) $H_D(s) = \dfrac{1.0}{1.0 + 0.1112\,s + 0.01499\,s^2}$

e) $H_E(s) = \dfrac{1.0}{1.0 + 0.1383\,s + 0.01499\,s^2}$

f) $H_F(s) = \left[\dfrac{31.83\,s}{1.0 + 31.83\,s}\right]^2$

g) $H_L(s) = \dfrac{1.0}{1.0 + 0.1592\,s} \cdot \dfrac{1.0}{1.0 + 1.592 \times 10^{[illegible]}\,s}$

h) $G_{SP}$

## LONG PERIOD FILTER TRANSFER FUNCTIONS

$H_{LP}(s) = G_{LP} \cdot H_A(s) \cdot H_B(s) \cdot H_C(s) \cdot H_D(s) \cdot H_E(s) \cdot H_F(s) \left(\frac{[illegible]}{[illegible]}\right)$

a) $H_A(s) = \left[\dfrac{1.0}{1.0 + 4.886\,s + 11.7\,s^2}\right]$

b) $H_B(s) = \dfrac{1.0}{1.0 + 0.9460\,s + 0.2398\,s^2}$

c) $H_C(s) = \dfrac{1.0}{1.0 + 0.6926\,s + 0.2398\,s^2}$

d) $H_D(s) = \dfrac{1.0}{1.0 + 0.28388\,s + 0.2398\,s^2}$

e) $H_E(s) = \left[\dfrac{31.83\,s}{1.0 + 31.83\,s}\right]^2$

f) $H_F(s) = \dfrac{1.0}{1.0 + 0.1592\,s} \cdot \dfrac{1.0}{1.0 + 1.592 \times 10^{-2}\,s}$

g) $G_{LP} = 32.0$

# APPENDIX C: PHASE AND GROUP DELAY WITH AFTAC FILTERS

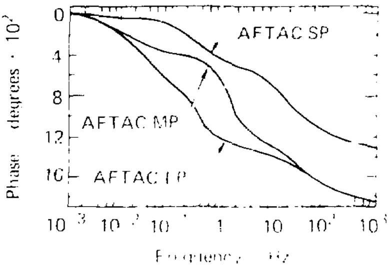


FIG. C1. Phase delay KS-36000 with AFTAC filters.

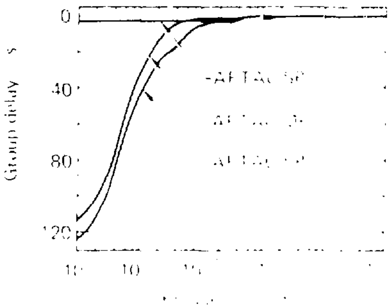


FIG. C2. Group delay KS-36000 with AFTAC filters.

# APPENDIX D: EVENT AMPLITUDE SPECTRA

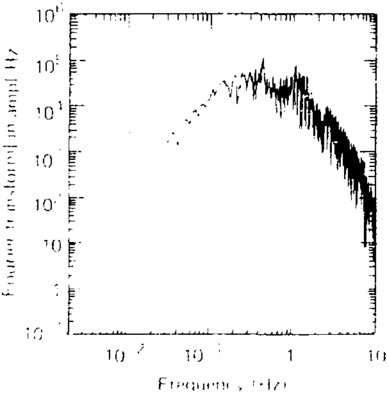

FIG. D1. Event (i): underground nuclear shot amplitude spectrum.

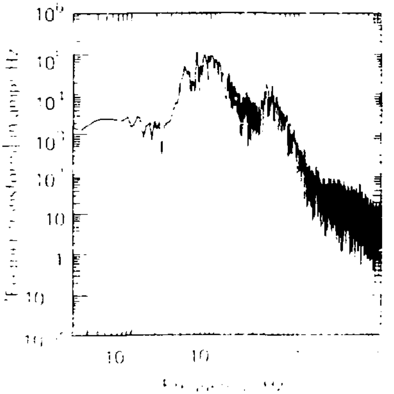

FIG. D2. Event (ii): regional earthquake amplitude spectrum.

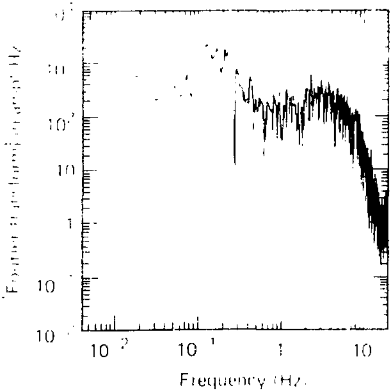


FIG. D3. Event (iii): local earthquake amplitude spectrum.

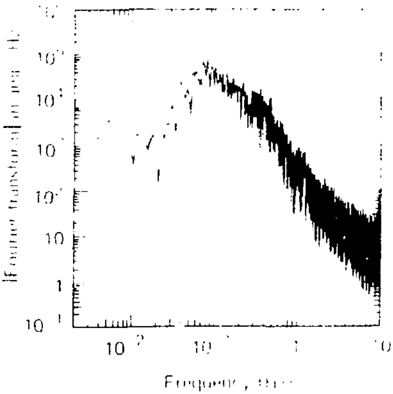

FIG. D4. Event (iv): large teleseism amplitude spectrum.